

RESEARCH ARTICLE | APRIL 22 1996

Dynamics of liquid acetone: Computer simulation

A. Bródka; T. W. Zerda



J. Chem. Phys. 104, 6313–6318 (1996)

<https://doi.org/10.1063/1.471271>



View
Online



Export
Citation

CrossMark



APL Quantum
Bridging fundamental quantum research with technological applications

Now Open for Submissions
No Article Processing Charges (APCs) through 2024

Submit Today



Dynamics of liquid acetone: Computer simulation

A. Bródka

Institute of Physics, University of Silesia, Uniwersytecka 4, 40-007 Katowice, Poland

T. W. Zerda

Physics Department, Texas Christian University, Fort Worth, Texas 76129

(Received 5 September 1995; accepted 17 January 1996)

Molecular dynamics simulations of liquid acetone are performed for the temperature range from 248 K to 323 K and pressures up to 2 kbar. The acetone molecule is modeled by four sites and intermolecular interactions are described by the optimized potential for liquid simulation (OPLS). The Ewald method and spherical truncation of the dipole–dipole interactions are used, and it is shown that both techniques give almost the same description of molecular motion. The calculated rotational relaxation times as well as translational diffusion coefficients satisfactorily agree with the experimental data. Rotational diffusion coefficients obtained from angular velocity correlation functions and rotational correlation times show anisotropy of reorientational motion of the acetone molecule. © 1996 American Institute of Physics. [S0021-9606(96)50516-3]

I. INTRODUCTION

In the last decade molecular dynamics (MD) simulation^{1,2} as well as the Monte Carlo method³ were used to investigate properties of liquid acetone. In those studies acetone was modeled by four Lennard-Jones (LJ) interaction centers and four partial charges. In the study of Ferrario *et al.*² the long-range electrostatic interactions were treated by the Ewald method⁴ whereas in the two other works^{1,3} the spherical truncation of the intermolecular interactions was used.

The paper by Evans and Evans¹ represents the most completed molecular dynamics study to date. However, one may find some inconsistencies in the calculations which makes their results unreliable. The LJ potential parameters were transferred from other molecules and the moments of inertia were 11%–16% smaller than the experimental data.^{5,6} Although the two other papers concentrate on aqueous mixtures² and organic solutes³ they also contain some results for pure acetone. Ferrario *et al.*² adjusted the LJ parameters and applied charges obtained from MINDO/3 calculations⁷ which yield a dipole moment of 2.71 D. For bulk acetone they reported thermodynamic properties, self-diffusion coefficient and rotational relaxation time τ_2 of the dipole moment at 298 K. The OPLS functions of Jorgensen *et al.*³ were determined through Monte Carlo simulation and the interaction model reproduced vaporization heat for acetone. It should be noted that the LJ potential parameters used in Refs. 2 and 3 are very similar, however, the OPLS charges give the dipole moment of 2.96 D, slightly higher than the experimental values of 2.90 D,⁵ 2.93 ± 0.03 D (Ref. 6) or 2.94 D.⁸

In the present paper the OPLS functions for acetone molecule³ are used in the MD simulations for the microcanonical ensemble (NVE). The calculations are carried out for a wide range of temperature and pressure, and the MD simulation results are compared with the experimental data. We focus our attention on the spherical truncation of the dipole–dipole interactions as this method can be adopted in studies of phenomena in nonisotropic systems, such as adsorption on

solid surface or in small pores. This work will serve as a starting point for further investigations of the dynamics of the acetone molecules in porous silica, and the results obtained here will help quantify differences between molecular behavior in restricted geometries and in the bulk phase. For selected thermodynamics states the calculations are repeated using the Ewald sum, and we compare results of these two methods.

II. MOLECULAR DYNAMICS SIMULATION

A molecule of acetone is represented by a rigid set of four interaction sites located on oxygen and carbon atoms. The geometry of the molecule is based on microwave results⁹ and the calculated principal moments of inertia; $I_x = 82.1 \times 10^{-47}$ kg m², $I_y = 98.5 \times 10^{-47}$ kg m², and $I_z = 170.2 \times 10^{-47}$ kg m² match the experimental values.^{5,6} The CH₃ groups are treated as unit sites, and the site locations in the molecular frame are presented in Table I. The interaction potential between α th and β th molecules is described in the standard form of the Lennard-Jones (LJ) potential plus dipole–dipole interaction represented by Coulomb interactions of fictitious partial charges

$$U_{\alpha\beta} = \sum_i \sum_j \left\{ 4\epsilon_{ij} \left[\left(\frac{\sigma_{ij}}{r_{ij}} \right)^{12} - \left(\frac{\sigma_{ij}}{r_{ij}} \right)^6 \right] + \frac{q_i q_j e^2}{4\pi\epsilon_0 r_{ij}} \right\}, \quad (1)$$

where i and j denote sites in the α th and β th molecules, respectively. The locations of charges q_i coincide with the LJ centers and they give a dipole moment of 2.96 D along the y axis of the molecular frame. All the parameters of the interaction potential³ are collected in Table I.

We simulate a system of 216 molecules in a cubic box of side L , and periodic boundary conditions are applied. The centers of the molecular masses are placed at nodes of a simple cubic structure, and orientations of the molecules are assigned randomly. Initial translational and angular velocities are random and consistent with the required temperature. The force and torque acting on a given molecule are calculated with a spherical cutoff radius $r_c = L/2$ which is applied

TABLE I. The interaction site locations in the molecular frame and the potential parameters for the acetone molecule.

Site	x (nm)	y (nm)	z (nm)	σ (nm)	ϵ/k_B (K)	q ($ e $)
C	0.0	0.008 93	0.0	0.375	52.87	0.300
O	0.0	0.131 12	0.0	0.296	105.75	-0.424
CH ₃	± 0.128 64	-0.069 60	0.0	0.391	80.57	0.062

to the centers of mass of the molecules. For the LJ interactions we use the shifted force potential, and the Coulomb interactions are multiplied by a Gaussian switching function which falls from 1 to 0 as distance between centers of mass of two acetone molecules increases from $0.95r_c$ to r_c .⁴ The standard long-range corrections for the LJ interactions⁴ are used and contribution to the energy for $r > r_c$ arising from the dipole-dipole interactions are calculated using effective spherically symmetrical potential function.¹⁰ Orientations are represented by quaternions.¹¹ The Newtonian and orientational equations of motions are solved using fifth- and fourth-order predictor-corrector methods,¹² respectively. The calculations are performed with a time step of 2.5 fs. In the equilibration run we carry out 5000 time steps during which velocities are scaled to obtain the required temperature. During the following 10 000 time steps, which constitutes the production stage, no further adjustments are made.

For selected thermodynamic states the calculations are repeated using the Ewald method to partial charges⁴ and assuming that the sphere built up of simulation boxes is immersed in dielectric continuum made of acetone and characterized by experimental electric permittivity.¹³

III. RESULTS AND DISCUSSION

Initially we performed the MD simulations for the liquid acetone at temperatures and densities along the saturated vapor curve. Thermodynamic states and some of the results obtained from the calculations for the spherical truncation of the interactions and the Ewald method are presented in Table II. In both cases fluctuations of temperature, pressure, and configurational energy are similar and their maximum errors

TABLE II. Temperatures, pressures, and configurational energies of liquid acetone along the saturated vapor curve. Values in parentheses refer to the Ewald method.

T (K)	ρ (g/cm ³)	p_σ (bar)	T^{MD} (K)	p^{MD} (bar)	$-U_\sigma^{\text{MD}}$ (kJ/mol)
293	0.789	0.234	298.1 (296.8)	623 (511)	29.4 (29.3)
323	0.754	0.786	324.2 (319.4)	448 (313)	27.7 (27.7)
353	0.719	2.148	358.8 (348.9)	302 (198)	26.1 (26.1)
383	0.679	4.803	377.2 (385.7)	58 (138)	24.7 (24.2)
413	0.634	9.454	420.3 (415.5)	120 (71)	22.5 (22.4)

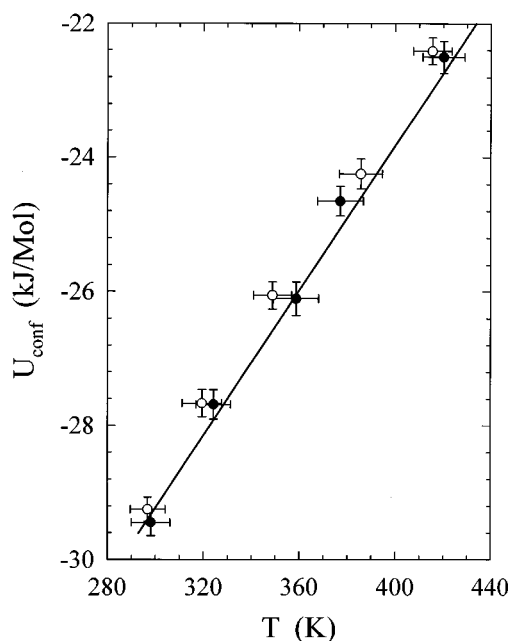


FIG. 1. Configurational energy of acetone along the saturated vapor curve as a function of temperature. Solid line represents values obtained from experimental data using Eq. (2), full and open circles are results of the MD simulations with the spherical truncation and Ewald method, respectively.

observed at the highest temperature are 9.5 K, 0.2 kbar, and 0.25 kJ/mol, respectively. Those values are similar to those reported by Haughney *et al.*¹⁴ for methanol. For both methods we did not observe any drift of temperature or the total energy. However, the spherical truncation of the interactions introduces fluctuations of the total energy which are 10 to 20 times larger than those for the Ewald method. For the spherical cutoff the total energy fluctuations are 0.5% and 1% at the lowest and the highest temperatures, whereas for the Ewald method the fluctuations are 0.03% and 0.1%, respectively.

The pressures obtained from the MD simulations are greater by about 0.5 kbar than the experimental values, particularly for lower temperatures (higher densities) where the differences are higher than the maximum pressure error. In Fig. 1 we compare the configurational energies obtained from the MD simulations with the values of the energy estimated from the experimental data for the latent heat of evaporation L_e ,¹⁵ the orthobaric molar volume V_σ ,^{15,16} the orthobaric pressure p_σ ,^{15,16} and temperature dependence of the second virial coefficient B ,¹⁷

$$U_\sigma \cong -L_e + p_\sigma \left[\left(\frac{RT}{p_\sigma} + B \right) - V_\sigma \right] - RT^2 \frac{dB}{dT} \left(\frac{RT}{p_\sigma} + B \right)^{-1}, \quad (2)$$

where R is the gas constant. This comparison shows that the potential parameters established by the OPLS method³ reproduce properly the internal energies of liquid acetone along the saturated vapor curve.

TABLE III. Thermodynamics states and MD simulations results. Values in parentheses refer to the Ewald method.

State number	T (K)	p (kbar)	ρ (g/cm ³)	T^{MD} (K)	p^{MD} (kbar)	$-U_{\text{conf}}^{\text{MD}}$ (kJ/mol)
1	248	0.001	0.843	250.9 (247.0)	0.97 (0.87)	32.1 (31.9)
2	273	0.001	0.815	276.2 (280.5)	0.80 (0.88)	30.6 (30.3)
3	298	0.001	0.786	302.0 (298.5)	0.57 (0.52)	29.3 (29.1)
3a		1.0	0.849	302.5	1.97	31.1
3b		2.0	0.891	298.5	3.35	32.2
4	323	0.001	0.757	328.6 (323.7)	0.43 (0.37)	27.8 (27.7)

Molecular dynamics of acetone is studied for four temperatures at atmospheric pressure, and at room temperature for pressures up to 2 kbar. The values of experimental densities corresponding to the simulated states were taken from Refs. 18 and 19, and they are listed in Table III. In the table there are also temperatures, pressures, and configurational energies obtained from the MD simulations. The configurational energy at 298 K (state 3) is almost the same as that reported by Ferrario *et al.*² Similarly as for the states along the saturated vapor curve, both methods of the MD simulation give pressures higher than experimental values, and the differences increase with density. Such behavior may suggest that the repulsive core of the intermolecular potential is too hard.

The rotational correlation functions

$$C_{1\alpha}(t) = \langle \cos[\mathbf{u}_{i\alpha}(t) \cdot \mathbf{u}_{i\alpha}(0)] \rangle, \quad (3a)$$

$$C_{2\alpha}(t) = \frac{1}{2} \langle 3 \cos^2[\mathbf{u}_{i\alpha}(t) \cdot \mathbf{u}_{i\alpha}(0)] - 1 \rangle, \quad (3b)$$

are calculated separately for each molecular axis $\alpha = x, y, z$. In the above equations $\mathbf{u}_{i\alpha}$ is a unit vector parallel to the α th molecular axis. The correlation functions are not shown here as they have typical shapes; Gaussian shape at short times and almost exponential decay at long times. The functions are integrated up to 15 ps and the rotational correlation times $\tau_{1\alpha}$ and $\tau_{2\alpha}$ are presented in Table IV. Following the analysis of computer experiment results developed by Zwanzig and Ailawadi²⁰ and Frenkel,²¹ the maximum errors of the reorientational relaxation times are 5% and 2% for the largest values of $\tau_{1\alpha}$ and $\tau_{2\alpha}$, respectively. The rotational relaxation times, $\tau_{1\alpha}$ or $\tau_{2\alpha}$, for the three axes of the molecular frame show reorientational anisotropy. Rotational correlation functions $C_{1\alpha}(t)$ and $C_{2\alpha}(t)$ for α th unit vector are influenced by reorientational motion around the two other axes. Rotation of the z axis describes pure tumbling motion of the molecule, whereas the correlation functions of the axes x and y contain contributions from both the tumbling and spinning motions. The first-order correlation times $\tau_{1\alpha}$ are almost three times greater than the second-order times $\tau_{2\alpha}$, $\alpha = x, y, z$. This behavior suggests that the Hubbard relation²² is fulfilled and the rotations may be treated as diffusional motions.

TABLE IV. Rotational correlation times of rank 1 and 2 obtained from MD simulations and experimental times obtained from Rayleigh scattering (Ref. 25), τ_2^{Ray} , and NMR measurements (Ref. 26), τ_r^{NMR} . Values in parentheses refer to the Ewald method.

State number	τ_{1x} (ps)	τ_{1y} (ps)	τ_{1z} (ps)	τ_{2x} (ps)	τ_{2y} (ps)	τ_{2z} (ps)	τ_2^{Ray} (ps)	τ_r^{NMR} (ps)
1	4.23 (4.28)	4.01 (4.09)	3.45 (3.60)	1.58 (1.60)	1.36 (1.40)	1.28 (1.31)
2	3.20 (3.08)	2.83 (2.62)	2.58 (2.29)	1.20 (1.07)	1.00 (0.88)	0.91 (0.80)
3	2.38 (2.56)	2.20 (2.38)	1.91 (1.96)	0.88 (0.91)	0.75 (0.80)	0.69 (0.69)	0.83	0.75
3a	3.29	2.89	2.57	1.29	1.04	0.96	1.15	...
3b	4.47	3.96	3.36	1.78	1.38	1.25	1.34	1.00
4	1.87 (2.07)	1.76 (1.79)	1.45 (1.69)	0.69 (0.73)	0.62 (0.64)	0.55 (0.58)

The rotational time τ_{1y} of dipole moment is a single particle microscopic time and cannot be compared directly with the macroscopic relaxation time τ_D obtained from the dielectric measurements.^{13,23} To estimate the molecular relaxation time τ_M it is necessary to consider a local field factor, and relation between τ_M and τ_D may be written as follows:²⁴

$$\tau_M = \frac{2\epsilon_s + \epsilon_\infty}{3\epsilon_s} \tau_D, \quad (4)$$

where ϵ_s and ϵ_∞ are the static and infinite-frequency dielectric permittivities, respectively. Using values of ϵ_s , ϵ_∞ , and τ_D for temperatures 283 K, 293 K, 303 K, and 313 K presented by Akhadov¹³ and for $T=293$ K reported by Vij *et al.*²³ one may calculate the molecular times τ_M . Figure 2 shows that the simulated times τ_{1y} match the values of τ_M .

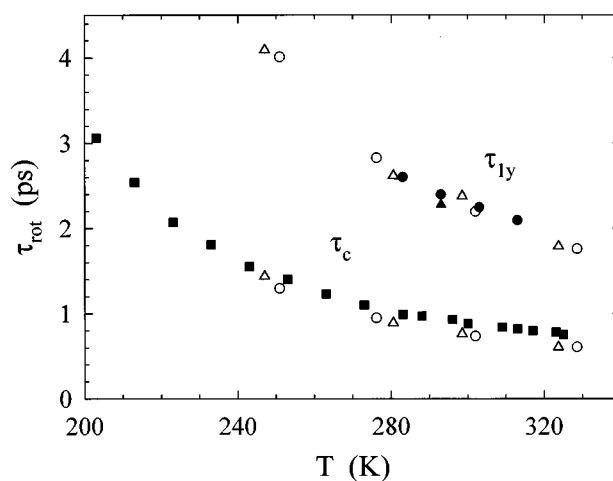


FIG. 2. Comparison of experimental and theoretical rotational correlation times for the dipole moment, τ_{1y} , and quadrupolar relaxation time, τ_c . Open circles and triangles denote results for the spherical truncation and Ewald method, respectively. Full symbols represent experimental data; circles and triangles, the molecular relaxation times τ_M (4) calculated on from data from Refs. 13 and 23, respectively, and squares, correlation times τ_c obtained from O¹⁷ NMR measurements (Ref. 30).

TABLE V. Angular velocity correlation times, $\tau_{\omega\alpha}$, rotational, D_α^r , and translational, D , diffusion coefficients. Values in parentheses refer to the Ewald method.

State number	$\tau_{\omega x}$ (ps)	$\tau_{\omega y}$ (ps)	$\tau_{\omega z}$ (ps)	D_x^r ($10^{10}/s$)	D_y^r ($10^{10}/s$)	D_z^r ($10^{10}/s$)	D^{msd} ($10^{-9} \text{ m}^2/s$)	D^{vcr} ($10^{-9} \text{ m}^2/s$)
1	0.046 (0.043)	0.045 (0.041)	0.058 (0.053)	19.2 (17.8)	16.0 (14.1)	11.7 (11.1)	1.53 (1.37)	1.55 (1.31)
2	0.055 (0.059)	0.057 (0.060)	0.071 (0.070)	25.7 (27.9)	22.0 (23.8)	15.8 (16.1)	2.17 (2.18)	2.23 (2.27)
3	0.064 (0.061)	0.067 (0.066)	0.083 (0.080)	32.5 (30.7)	28.4 (27.7)	20.2 (19.4)	3.04 (3.02)	3.10 (2.98)
3a	0.049	0.048	0.061	25.1	20.2	14.9	1.76	1.76
3b	0.039	0.036	0.046	19.4	15.2	11.1	1.28	1.26
4	0.074 (0.075)	0.078 (0.077)	0.093 (0.090)	40.7 (40.8)	35.9 (34.9)	25.7 (24.6)	4.63 (4.54)	4.56 (4.46)

In Table IV we list available experimental times obtained from orientational parts of the depolarized Rayleigh scattering intensities,²⁵ τ_2^{Ray} , and from intramolecular part of the spin-lattice relaxation times T_1 measured on hydrogens,^{26,27} τ_2^{NMR} . The values of τ_2^{Ray} calculated from the limiting slope of the rotational correlation function coincide with the rotational relaxation times for the dipole moment τ_{2y} , which indicates that MD simulations nicely reproduce pressure dependence of molecular rotations. The agreement between NMR data and MD simulation results is not as good. τ_2^{NMR} time shows pressure dependence weaker than the simulated relaxation times, which may be attributed to the contributions from relatively free rotations of the methyl groups. The spinning motion of the CH_3 group is affected by increased density to a lesser degree than rotations of the whole molecule,^{26,27} and this effect may explain observed discrepancies.

We calculated three components of the angular velocity correlation functions $C_{\omega\alpha}(t)$, $\alpha = x, y, z$, and integration of these functions gives the correlation times $\tau_{\omega\alpha}$, $\alpha = x, y, z$, which are collected in Table V. The maximum statistical uncertainties^{20,21} of the angular velocity correlation times are less than 1%. The times $\tau_{\omega x}$ and $\tau_{\omega y}$ have similar values suggesting that acetone can be treated as a symmetric top molecule. However, anisotropy of rotational motion is better characterized by rotational diffusion coefficients D_α^r defined as^{28,29}

$$D_\alpha^r = \frac{k_B T}{I_\alpha} \tau_{\omega\alpha}, \quad \alpha = x, y, z, \quad (5)$$

where $\tau_{\omega\alpha}$ is the angular velocity correlation time and I_α is the moment of inertia for the α th axis (see Table V). The spinning motion, i.e., rotation around the z axis, is less hindered. D_x^r and D_y^r describe the tumbling motions, but rotation about the x axis is connected with a change of the dipole moment orientation and thus it is restricted more than rotation about the y axis. With increasing density (increasing pressure or decreasing temperature) the rotational anisotropy increases. The above results indicate that the difference between the moments of inertia I_x and I_y is crucial and leads to

different rotational coefficients D_x^r and D_y^r . Equality of D_x^r and D_y^r , suggested by Ancian *et al.*,³⁰ is a result of the assumption $I_x \approx I_y$.

Diffusion coefficients for rotational motion may be used to estimate the effective rotational times for quadrupolar relaxation τ_c . In our calculations we assume that orientation of the electric gradient tensor in the acetone molecule is the same as for formaldehyde;^{31,32} the largest gradient tensor component is in the plane of the molecule and perpendicular to the $\text{C}=\text{O}$ bond, i.e., it is lying along the x axis. Therefore, in the theoretical expression for a planar asymmetric rotor describing τ_c [Eqs. (4.4) in Ref. 28 and Eq. (5.5) in Ref. 29] one puts $\phi=0$ and the time τ_c has the following form:

$$\tau_c = \frac{4D_x^r + (\eta - 1)^2 D_y^r + (\eta + 1)^2 D_z^r}{12(D_x^r D_y^r + D_x^r D_z^r + D_y^r D_z^r)}, \quad (6)$$

where $\eta = (q_y - q_z)/q_x$ is the field gradient asymmetry parameter. Unfortunately, the value of η for acetone is unknown and instead we used the value for formaldehyde $\eta = 0.6944$.³¹ In Fig. 2 these times are compared with the experimental times obtained from O^{17} NMR measurements.³⁰ The theoretical values are slightly smaller than the experimental times τ_c . However, they reproduce very well experimentally observed temperature dependence of τ_c .

To characterize translational motion we calculate the velocity correlation functions and mean square displacements which are used to estimate the diffusion coefficients,³³

$$D^{\text{vcr}} = \frac{1}{3} \int_0^\infty \langle \mathbf{v}(t) \cdot \mathbf{v}(0) \rangle dt, \quad (7a)$$

$$D^{\text{msd}} = \lim_{t \rightarrow \infty} \frac{1}{6t} \langle |\mathbf{r}(t) - \mathbf{r}(0)|^2 \rangle. \quad (7b)$$

The diffusion coefficients are calculated from positions and velocities of the molecular centers of mass and their maximum errors^{20,21} do not exceed 2%. The results collected in Table V show that both methods give almost the same values, and the diffusion coefficient for the state 3 is almost identical as that reported by Ferrario *et al.*² In Figs. 3 experimental diffusion coefficients^{26,27,34-38} are compared with the values obtained from the MD simulations. It is seen that the

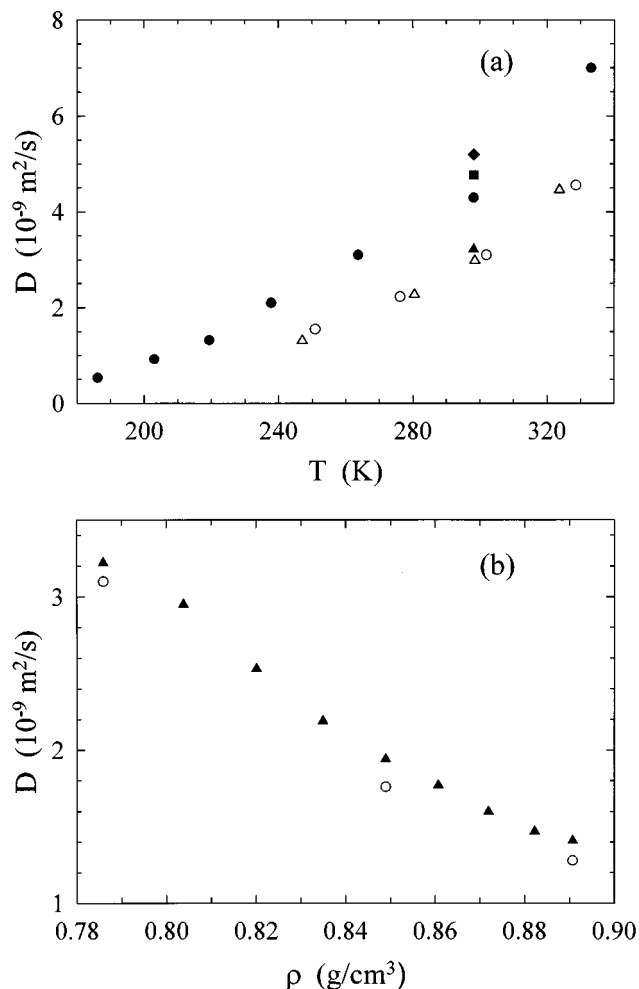


FIG. 3. Temperature (a) and density (b) dependencies of the translational diffusion coefficient. Open symbols, MD results using the spherical truncation (circles) and Ewald method (triangles). Full symbols, experimental values; circles, Ref. 36; squares, Ref. 34; diamonds, Ref. 38; and triangles, Eq. (8) and results from Refs. 26 and 27.

theoretical values properly describe temperature and density dependencies of the diffusion coefficient. However, they are about 30% smaller than most of the experimental diffusion coefficients, compare Fig. 3(a), obtained from the NMR spin-echo techniques^{34–36} and spin-lattice relaxation time T_1 measurements.^{37,38} On the other hand, in Fig. 3(b) one observes a very good agreement between the simulated coefficients and values of D calculated from the translational relaxation times τ_t (Refs. 26 and 27) applying the following formula:^{39,40}

$$D = \frac{2a^2}{\tau_t}, \quad (8)$$

where a is the mean radius of the molecule, and for acetone $a = 0.278$ nm.²⁶ The relaxation time τ_t is the time for a molecule to diffuse one molecular diameter, and its values were calculated from the intermolecular part of the NMR spin-lattice relaxation time T_1 measured on hydrogens^{26,27} using Hubbard's theory.³⁹ That theory takes into account that hy-

drogen atoms are distanced from the center of mass of polyatomic molecule and rotations contribute to the intermolecular relaxation time T_1 .

IV. CONCLUSIONS

The potential parameters for the acetone molecule applied originally in Monte Carlo simulation³ are used in MD simulations. The interaction model properly reproduces configurational energies of liquid acetone along the saturated curve and it is capable of providing a good description of molecular motion for a wide range of temperature and pressure. The rotational relaxation times of the first and second rank as well as the rotational diffusion coefficients show relatively strong anisotropy of reorientational motion, and this anisotropy increases with density. The simulations are performed using the Ewald sum which correctly calculates the long range forces and the spherical truncation technique. Apart from the fact that the spherical truncation introduces fluctuations of the total energy an order of magnitude larger than the Ewald method, both methods give the same description of the molecular dynamics. This observation maybe helpful in the simulation of systems for which the periodic boundary conditions must be abandoned, for example in a study of nonisotropic systems such as a polar fluid on a solid surface or in small pores. In such a case, the Ewald method cannot be used, however, one may apply the spherical truncation of the dipole–dipole interactions.

ACKNOWLEDGMENTS

This work was supported by KBN Grant No. 3T09C03608. The donors of the Petroleum Research Foundation administrated by the American Chemical Society are also acknowledged.

- ¹G. J. Evans and M. W. Evans, *J. Chem. Soc. Faraday Trans. 2* **79**, 153 (1983); M. W. Evans and G. J. Evans, *Adv. Chem. Phys.* **63**, 377 (1985).
- ²M. Ferrario, M. Haughney, I. R. McDonald, and M. L. Klein, *J. Chem. Phys.* **93**, 5156 (1990).
- ³W. L. Jorgensen, J. M. Briggs, and M. L. Contreras, *J. Phys. Chem.* **94**, 1683 (1990).
- ⁴M. P. Allen and D. J. Tildesley, *Computer Simulation of Liquids* (Clarendon, Oxford, 1989).
- ⁵J. D. Swalen and C. C. Costain, *J. Chem. Phys.* **31**, 1562 (1959).
- ⁶R. Peter and H. Dreizler, *Z. Naturforsch.* **20a**, 301 (1965).
- ⁷C. A. Wellington and S. H. Khouwaiter, *Tetrahedron* **34**, 2183 (1978).
- ⁸M. T. vonRätzsch, C. Wohlforth, U. Credo, A. Jarmuschewitsch, and U. Nehmer, *Z. Phys. Chem.* **257**, 161 (1976).
- ⁹R. Nielson and L. Pierce, *J. Mol. Spectrosc.* **18**, 344 (1965).
- ¹⁰J. O. Hirschfelder, C. F. Curtis, and R. B. Bird, *Molecular Theory of Gases and Liquids* (Wiley, New York, 1954), p. 28.
- ¹¹D. J. Evans and S. Murad, *Mol. Phys.* **34**, 327 (1977).
- ¹²C. W. Gear, *Numerical Initial Value Problems in Ordinary Differential Equations* (Prentice–Hall, Englewood Cliffs, 1971).
- ¹³Y. Y. Akhadov, *Dielectric Properties of Binary Solutions* (Pergamon, Oxford, 1980), pp. 325, 326.
- ¹⁴M. Hughney, M. Ferrario, and I. R. McDonald, *J. Phys. Chem.* **91**, 4934 (1987).
- ¹⁵R. W. Gallant, *Hydrocarbon Processing* **47/8**, 127 (1968).
- ¹⁶*International Critical Tables* (Maple, New York, 1928), Vol. 3, p. 239.
- ¹⁷J. H. Dymond and E. B. Smith, *The Virial Coefficients of Pure Gases and Mixtures* (Clarendon, Oxford, 1980), p. 90.
- ¹⁸W. Schindler, P. T. Sharko, and J. Jonas, *J. Chem. Phys.* **76**, 3493 (1982).

- ¹⁹ Landolt–Börnstein: *Densities of Liquid Systems*, New Series (Springer, Berlin, 1974), Vol. IV/1a, p. 225.
- ²⁰ R. Zwanzig and N. K. Ailawadi, *Phys. Rev.* **182**, 280 (1969).
- ²¹ D. Frenkel, in *Intermolecular Spectroscopy and Dynamical Properties of Dense Systems, Proceedings of the International School of Physics “Enrico Fermi”* (North-Holland, Amsterdam, 1980), Vol. 75, p. 156.
- ²² P. S. Hubbard, *Phys. Rev.* **131**, 1155 (1963).
- ²³ J. K. Vij, T. Grochulski, A. Kocot, and F. Hufnagel, *Mol. Phys.* **72**, 353 (1991).
- ²⁴ C. J. F. Bötcher and P. Bordevijk, *Theory of Electric Polarization* (Elsevier, Amsterdam, 1978), Vol. II, p. 162.
- ²⁵ J. F. Dill, T. A. Litovitz, and J. A. Bucaro, *J. Chem. Phys.* **62**, 3839 (1975).
- ²⁶ T. E. Bull and J. Jonas, *J. Chem. Phys.* **52**, 4553 (1970).
- ²⁷ T. E. Bull and J. Jonas, *J. Chem. Phys.* **52**, 2779 (1970).
- ²⁸ W. T. Huntress, Jr., *J. Chem. Phys.* **48**, 3524 (1968).
- ²⁹ W. T. Huntress, Jr., *Adv. Magn. Reson.* **4**, 1 (1970).
- ³⁰ B. Ancian, B. Tiffon, and J.-E. Dubois, *Chem. Phys.* **74**, 171 (1983).
- ³¹ W. H. Flygare and J. T. Lowe, *J. Chem. Phys.* **43**, 3645 (1965).
- ³² C. P. Cheng and T. L. Brown, *J. Am. Chem. Soc.* **101**, 2327 (1979).
- ³³ J. P. Hansen and I. R. McDonald, *Theory of Simple Liquids* (Academic, London, 1986).
- ³⁴ D. W. McCall, D. C. Douglass, and E. W. Anderson, *J. Chem. Phys.* **31**, 1555 (1959).
- ³⁵ D. W. McCall and D. C. Douglass, *J. Phys. Chem.* **71**, 987 (1967).
- ³⁶ G. J. Krüger and R. Weiss, *Z. Naturforsch.* **25a**, 777 (1970).
- ³⁷ M. D. Zeidler, *Ber. Bunsenges. Phys. Chem.* **69**, 659 (1965).
- ³⁸ E. von Goldammer and M. D. Zeidler, *Ber. Bunsenges. Phys. Chem.* **73**, 4 (1969).
- ³⁹ P. S. Hubbard, *Phys. Rev.* **131**, 275 (1963).
- ⁴⁰ J. G. Powles, M. Rhodes, and J. H. Strange, *Mol. Phys.* **11**, 515 (1966).